

An Example for Arc-Type Granitoids along Collisional Zones: The Pertek Granitoid, Taurus Orogenic Belt, Turkey

Sevcan Kürüm^{1*}, Bünyamin Akgül¹, Ayten Öztüfekçi Önal², Durmuş Boztuğ², Yehudit Harlavan³, Melek Ural¹

¹University of Fırat, Engineering Faculty, Department of Geology, Elazığ, Turkey

²University of Tunceli, Engineering Faculty, Department of Geology, Tunceli, Turkey

³Geological Survey of Israel, Jerusalem, Israel

E-mail: *skurum@firat.edu.tr

Received April 5, 2011; revised June 8, 2011; accepted July 14, 2011

Abstract

The Pertek granitoid consisting dominantly of diorite, quartz diorite, quartz monzodiorite, tonalite and lesser granite, adamellite and syenite, is considered to form the easternmost continuation of the Central Anatolian Crystalline Complex. Diorite and monzonites of this granitoid complex are cut by the granitic dykes. The Pertek granitoid, in the study area, is found in the Permo-Triassic Keban metamorphic sequence along intrusive and tectonic contacts. Along the intrusive contacts metasomatic mineralizations are common. Granitoids are, depending on the mineralogical composition, low-, middle- high-K subalkaline features. Major oxide-SiO₂ variation diagrams show that fractionation (particularly plagioclase, hornblende, pyroxene and olivine fractionation) played an important role on the granitoid formation during a continuous crystallization process. Distribution of the samples from the Pertek granitoid in the tectonic setting diagrams, and their chondrite- and primordial mantle-normalized trace element patterns resemble to the of arc-type granitoids. Trace element and rare earth element compositions indicate that the magma, from which the Pertek granitoid crystallized, derived from a mantle that was enriched by the fluids derived from the subducted slab, however this magma was contaminated by the crust during its intrusion. These geochemical characteristics are also supported by the field observations. The field and geochemical characteristics of the Pertek Granitoid suggest that they are similar to the other granitoids cropping out in the central and eastern Anatolia and they form the lateral continuation of the same magmatic belt.

Keywords: Pertek, Tunceli, Island Arc, Granitoid, Geochemistry

1. Introduction

E-SE Anatolia Orogenic Belt was formed along the collision zone between Afro-Arabian and Eurasian plates during the Middle Miocene [1,2]. Palaeozoic-Mesozoic platform-type carbonates, supra-subduction zone ophiolites and granitoids are found together and form the tectono-magmatic units of this belt. Isotopically dated granitoids of this belt yield a Cretaceous-Eocene age [3,4,2]. These granitoids are considered to be formed along the southern Neo-Tethyan subduction in the larger-scale Neo-Tethyan Conversion System and expose in three different areas. From west to east, in the collision zone, Afşin-Elbistan (Kahramanmaraş), Doğanşehir (Malatya) and

Baskil-Keban (Elazığ) granitoids have been studied in detail and results have been published [5-17,3,18].

The Pertek granitoid, in a similar fashion to the other granitoids along this belt, show intrusive contacts with the Palaeozoic-Mesozoic Keban metamorphics (Keban platform-type carbonates). Platform-type carbonates were thrust onto the granitoids by the Eocene aged and younger tectonic activity to form the tectonic contact observed between the granitoids and the older metamorphic sequence [19]. Both the basement units and the Pertek Granitoid, in the study area, are overlain by the Tertiary marine sediments, terrestrial volcanic rocks and equivalent terrestrial sediments [20] (**Figure 1**).

In this study, field occurrences, petrographical and geo-

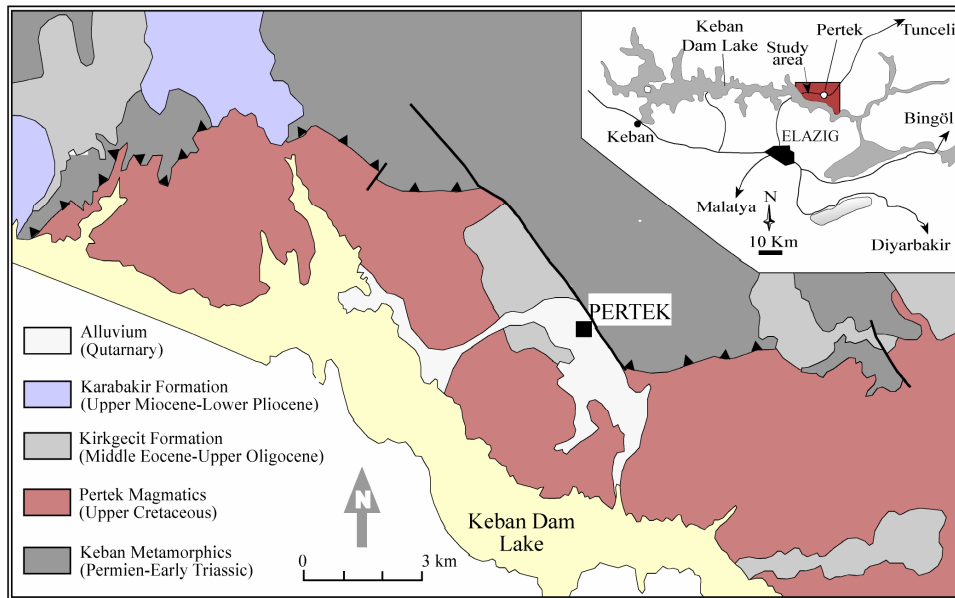


Figure 1. Location map of the study area and Geological map of the Pertek granitoid (simplified) [21].

chemical characteristics of the Pertek granitoid are documented for the first time. Results of this study will discuss the tectonic setting and source of the magmatic rocks in the area and contribute to the understanding of the geological evolution of the region. This contribution would also explain to the future researchers that using only geochemical data in order to evaluate the geological evolution of the region may result in erroneous interpretations.

2. Analytical Techniques

The geological maps [21] covering the area where Pertek granitoid crops out were used in this study and they were revised whenever needed. Samples were taken from different rock units in relatively fresh parts of the units. Of those, 45 samples were examined under polarized microscope. Totally 34 samples were geochemically analysed 29 of them in ACME Laboratories (Canada) and 5 of them in ACTLAB (Canada) and their major element oxide, trace element and rare earth element contents were determined.

3. Regional Geology

SE Anatolian Orogenic Belt was controlled by the opening of southern branch of the Neo-Tethys Ocean from Late Triassic to Early Cretaceous between the Keban Platform and Pütürge metamorphics [22] and following northward subduction under the Keban Plate during Senomanian-Turonian. Yazgan and Chessex [8] suggested that Eastern Tauride tectonism developed as an arc-continent collision

between Keban and Arabic microcontinents that started in Late Cretaceous-Early Maastrichtian and continued until Early Eocene. Magmatic rocks observed in this orogenic belt formed along an arc that developed on oceanic and continental crust in Malatya Province and westward [22,6]. A number of researchers [8,1,9,12,4,14] documented that this magmatic belt consists of calc-alkaline volcanic and plutonic rocks.

Palaeozoic-Mesozoic Keban metamorphics form the oldest units in the study area. The Keban metamorphics consist of marble, chalk schist and amphibolites and bound the magmatic rocks along their northern side (**Figure 1**) in the study area. Kipman [23], suggested that the Keban metamorphics are Jurassic-Early Cretaceous in age and metamorphosed under low P-T conditions. Yazgan [22] on the other hand suggested that the platform-type carbonates in this metamorphic sequence metamorphosed under greenschist metamorphism conditions during Senomanian along the subduction zone. Özgül and Turşucu [24] also suggested greenschist conditions for the metamorphism of the Keban metamorphics supporting Yazgan's view [22]. Some researchers [6,9] on the other hand proposed that the arc magmatism caused the metamorphism. Intrusive contact between the arc magmatics and metamorphics and mineralizations along this intrusive contact has been previously documented by various researchers. [22,10,18,25].

The Pertek granitoid crops widely crop out in the northern and southern part of the Keban Dam to the north of Elazığ. The Pertek granitoid is overlain by the Eocene-Oligocene marine sediments and Miocene-Pliocene

terrestrial volcanic and sedimentary sequences.

4. Field Characteristics

The Pertek pluton crops out widely along two opposite sides of the Keban Dam Lake situated to the North of Elazığ, therefore appears like two different plutons in the field. In this study is focused on the northern side of the dam lake (**Figure 1**) where the magmatic rocks consist of diorite-gabbro, quartz diorite, tonalite, monzonites and cross-cutting dykes of acidic composition. These different units are not indicated in geological map, however diorites crop out widely along the study area, whereas tonalites have wide outcrops in western parts of the study area. Monzonites, on the other hand, volumetrically dominates the outcrops to the south of Pertek.

In the field, diorites are weathered, medium-grained, competent, dark gray-black in appearance and form a smooth topography. Tonalites consist of large quartz crystals, less amount of mafic minerals and more mafic microgranular enclaves (MME). To the west of Pertek, close to the carbonates of the surrounding metamorphic association, strong hydrothermal alteration and oxidation in mafic minerals are common. Prolonged amphiboles which are found along the intrusive contacts may indicate a skarn zone. Presence of skarn metamorphism in the region has previously been noted by Altunbey and Çelebi [25]. Mafic microgranular enclaves, preserved in the main pluton, are generally rounded and ellipsoidal in shape and reach up to 50 cm in diameter. Dioritic main body is cross cut by the harder, felsic, fine grained, acidic and strongly altered porphyres that are exhumed widely in the north of Pertek and its thickness vary from a few meters to few hundreds meters. In the southeastern part of Pertek, close to the Keban Dam Lake, monzonites are less altered than the other magmatic lithologies. Monzonites are easily distinguished in the field because of containing pink K-feldspar crystals which display lengths from a few millimeter to a few centimeters. Monzonites are not mappable in scale and generally found as small stocks cutting diorites and tonalites in the lower parts and a few tens of meter-thick dykes, in the upper parts. At the 30th km of Pertek-Tunceli highway, in a valley, up to 3 m-thick, hard, NW-SE-trending, almost vertical aplite dykes are also found in the upper part of the magmatic body. In the uppermost part of these dykes cataclastic enclaves are commonly found.

The Kırgeçit formation cropping out in the study area is represented by sandstone-mudstone alternation and channel-fill conglomerates [19]. The Late Miocene-Pliocene aged Karabakır formation which is dominated by the pyroclastic rocks and lava flows in the study area, forms the youngest unit and crops out in the N-NW part

of the study area.

The thrust fault along which the Keban metamorphics are found tectonically overlying the Pertek magmatics, form the main tectonic structure in the study area (**Figure 1**). [19] suggested that this approximately 10° north dipping fault is Late Cretaceous - Late Palaeocene in age. NW-SE trending strike-slip fault which is observed in the west of Pertek, is another significant tectonic structure in the area (**Figure 1**).

5. Petrography

Petrographically the Pertek granitoid consists of quartz diorite, tonalite-granite/granodiorite, monzonite, diorite/gabbro. Samples are dominantly plotted in quartz diorite, diorite quartz monzodiorite and tonalite areas in nomenclature diagram [26] and only one sample is found in granite, ademellite and syenite areas respectively (**Figure 2**). Places of the samples in the geochemical nomenclature diagrams are in accordance with the petrographic nomenclature. Sample PR-20 is plotted in the geochemical nomenclature diagram in granite area, PR-31 in syenite area and PR-26 in ademellite area and they are found in Streckeisen [27] triangle diagram in monzogranite area.

Diorites and quartz diorites are fine to medium grained granular and poikilitic in texture and are dominated by plagioclase and hornblende crystals. In some of the samples hornblends are greater in amount than the plagioclases. Plagioclases in diorites commonly show un-equilibrium textures of oscillatory zoning and polysynthetic twinning indicating open system processes like magma mixing [28]. Subhedral or skeleton shaped hornblends with green pleochroism are commonly chloritized. Poikilitic texture is characterized in hornblends by plagioclase and opaque mineral inclusions. In some hornblende crystals relic pyroxenes are observed indicating that hornblends were formed by uralitization in pyroxenes.

Tonalite, granite and granodiorites are coarse grained hypidiomorphic granular in texture. Plagioclase, quartz, amphibole, K-feldspar, apatite, zircon, sphene and opaque minerals form the mineral association. Plagioclases are the dominant felsic minerals and show albite twinning, zoning and overgrowth texture. Quartz crystals are varying in size, unihedral and show wavy extinction. Amphiboles show green pleochroism. Chloritization and opacification in amphiboles and argillic alteration in K-feldspars are the common alteration types. Sphenes are found as coarse idiomorphic crystals and apatites as acicular crystals in accessory phase. Zircon is rarely observed.

In monzonites plagioclase, amphibole, quartz and K-feldspar form the main mineral phase. Amphiboles with

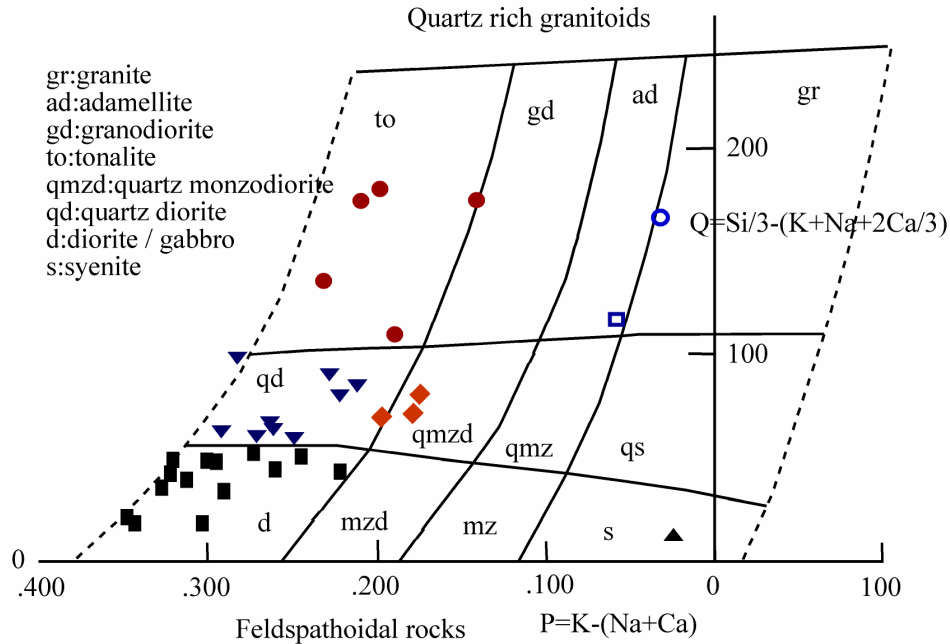


Figure 2. QP plot [26] for samples from the Pertek granitoid.

slight, pale green pleochroism are rarely found as coarse crystals but commonly as pseudomorphic acicular crystals. Chloritization is the common alteration type.

Sample PR-31 is distinguishable from the remaining sample even as hand specimen. Large amount of perthitic K-feldspar crystals give a pink color to the syenites in hand specimen. The main minerals forming the rock are perthitic K-feldspars. Quartz content of the Syenites is low.

6. Geochemistry

Whole rock geochemical composition of 34 samples from the Pertek granitoid is given in **Table 1** and results are plotted in total alkalis-Silica (**Figure 3(a)**) and AFM (**Figure 3(b)**) diagrams. All samples, except for syenite (PR 31), are gathered in subalkaline area in total alkalis-silica diagram. Diorite/gabbro and quartz diorite samples are mostly tholeiitic-high Mg and other samples are calc-alkaline in nature. In AFM diagram quartz monzodiorites and granites are found in high K area and other samples are found in low K area. According to Shand index samples are metaluminous in character ($A/CNK = -0.5 - 1$; $A/NK < 1$) and I-type in nature ($A/CNK < 1.1$) [29]. The I-type nature of the samples is in accordance with the mafic mineral assemblage.

In Harker-type variation diagrams, it is distinguished that the Pertek granitoid evolved from a single magma phase during continuous normal fractional crystallization stage. During this crystallization stage mineral fractionation did not develop in diorites, less developed in

quartz diorites and well developed in tonalites. Additionally, while, depending on the mafic composition, enrichment in FeO^* , MgO , CaO_2 and Ti_2O ratios is observed in diorites (**Figure 4(b), (c), (d), (g)**); enrichment in Na_2O ratio are observed depending on the K-feldspar (**Figure 4(e)**) in tonalites and quartz monzodiorites.

In the chondrite-normalized spider diagrams (**Figure 5(a), (c), (e)**), diorites and quartz diorites show similar patterns (**Figure 5(a), (c)**). In both groups, some of the samples are depleted in LREEs and others are enriched. In these diagrams, in some of the diorite and quartz diorite samples, depletion in LREEs is more significant than the others. In these samples depletion in HREEs is also more distinguishable compared to the others. In depleted LREEs samples a significant enrichment of Eu is observed. In addition to the similar REE patterns of diorite and quartz diorite samples, a concave pattern from the enriched LREEs to depleted HREEs is observed (**Figure 5(a), (c), (e)**). The REE composition of samples indicate a fractionation processes in these rocks [30].

In the Primordial mantle-normalized spider diagrams (**Figure 5(b), (d), (f)**) diorites and quartz diorites show two different patterns in LILEs (K, Rb, Ba, Th) (**Figure 5(b), (d)**). An enrichment in LILEs in the other rock groups, on the other hand, is clear (**Figure 5(f)**). Significant enrichment in LILEs may indicate an E-MORB or within plate setting for the basic rocks [31]. In the acidic rocks, however, enrichment in LILEs may indicate either crustal contamination [32] or enrichment by fluids derived from the oceanic crust [33]. In these diagrams, Nb show

Table 1. Major (%) and trace element (ppm) contents of the Pertek granitoides.

Sample Symbol	PR1	PR29	PR32	PR2	PR3	PR5	PR8	PR9	PR10	PR13	PR15	PR16	PR19	PR25	PR27	PR28	PR30
SiO ₂	56.11	63.14	62.94	48.26	44.40	46.22	46.43	46.80	46.34	44.95	46.60	48.12	47.65	54.89	49.98	50.85	56.68
Al ₂ O ₃	13.73	17.84	17.69	17.36	16.44	16.50	21.78	17.93	14.73	17.29	14.24	15.53	14.70	17.86	18.05	20.33	17.69
Fe ₂ O ₃	7.09	4.13	4.58	11.44	11.24	8.66	5.64	5.80	12.87	7.54	8.82	7.54	7.46	7.24	10.10	7.09	6.85
MgO	3.52	1.16	1.25	6.24	7.45	8.86	6.67	10.84	7.84	11.51	12.27	9.99	11.46	4.31	5.60	4.50	3.14
CaO	7.79	4.36	4.70	11.08	12.6	15.73	15.59	15.13	14.19	12.69	13.31	13.88	14.80	7.99	9.66	10.95	7.07
Na ₂ O	2.86	4.85	4.47	2.18	2.21	1.39	1.49	1.24	1.36	1.45	1.41	1.73	1.25	4.10	2.64	2.97	4.12
K ₂ O	2.67	3.18	3.10	0.49	0.52	0.12	0.07	0.05	0.10	0.10	0.19	0.11	0.07	1.42	1.22	0.90	2.40
TiO ₂	0.32	0.28	0.30	0.84	0.58	0.42	0.16	0.18	1.42	0.36	0.43	0.34	0.36	0.52	0.72	0.47	0.48
P ₂ O ₅	0.10	0.09	0.09	0.06	0.06	0.02	<0.01	<0.01	0.03	0.01	0.02	<0.01	0.01	0.08	0.09	0.06	0.11
MnO	0.16	0.09	0.007	0.18	0.19	0.16	0.11	0.10	0.16	0.12	0.18	0.14	0.13	0.13	0.15	0.12	0.13
LOI	5.5	0.7	0.6	1.6	4.6	1.7	1.9	1.7	1.2	3.7	2.2	2.3	1.7	1.3	1.5	1.5	1.1
Total	99.84	99.80	99.78	99.74	99.78	99.79	99.84	99.79	99.71	99.78	99.75	99.78	99.73	99.78	99.70	99.79	99.76
K ₂ O/P ₂ O ₅	26.70	35.33	34.44	8.17	8.67	6.00	7.00	5.00	3.33	10.00	9.50	11.00	1.00	17.75	13.56	15.00	21.82
A/CNK	0.51	0.59	0.59	0.56	1.07	0.49	1.27	1.09	0.94	1.21	0.96	0.99	0.91	1.32	1.34	1.37	1.30
A/NK	2.48	2.22	2.34	6.50	6.02	10.93	13.96	13.90	10.09	11.15	8.90	8.44	11.14	3.24	4.68	5.25	2.71
Ni (ppm)	<20	21	<20	22	<20	62	41	78	41	148	133	109	196	22	78	<20	<20
Sc	7	5	4	35	26	52	41	40	57	27	37	58	51	16	31	26	10
Cs	2.1	2.8	1.2	0.1	0.8	0.1	<0.1	<0.1	0.2	0.1	0.2	0.2	0.3	2.0	3.2	5.9	1.0
Ga	14.8	16.8	16.6	16.4	14.5	12.8	13.9	10.3	15.3	11.8	10.0	12.1	10.5	17.3	17.1	16.3	16.8
Hf	3.5	4.6	4.1	1.7	0.9	0.7	0.3	0.3	0.6	0.5	0.6	0.3	0.3	2.7	2.2	1.7	3.0
Sn	1	1	<1	<1	<1	1	<1	<1	<1	<1	<1	4	<1	1	<1	1	1
Ba	361	835	1019	137	98	23	14	8	9	12	20	13	7	471	512	288	713
Rb	77.8	88.2	79.8	6.0	16.1	2.4	1.0	1.0	1.1	1.4	6.4	1.2	1.1	48.3	24.8	19.6	65.0
Sr	243	464	548	257	289	193	222	174	226	150	179	156	145	487	467	677	631
Nb	9.9	17.6	11.6	3.1	3.2	0.8	0.2	0.2	0.2	0.5	0.5	0.2	<0.1	7.8	8.6	8.8	10.6
Zr	124.6	190.0	184.9	60.9	32.4	15.6	8.5	3.6	19.1	14.8	17.8	7.9	8.5	112.0	76.2	59.3	130.4
Ta	0.5	1.4	1.1	0.2	0.2	<0.1	<0.1	<0.1	<0.1	<0.1	<0.1	<0.1	<0.1	0.3	0.8	0.8	0.6
Th	4.5	19.6	11.3	1.8	0.7	0.2	<0.2	<0.2	<0.2	<0.2	<0.2	<0.2	<0.2	10.2	3.7	6.8	9.0
U	1.9	3.9	3.4	0.8	0.4	0.1	0.1	<0.1	<0.1	0.1	0.2	<0.1	<0.1	3.1	1.8	2.8	3.9
V	44	38	51	374	247	239	150	115	715	115	160	185	197	151	317	151	116
W	50.5	3.3	2.0	<0.5	37.1	5.1	1.8	1.1	<0.5	6.1	1.7	3.3	<0.5	1.5	<0.5	3.3	1.1
Y	21.5	16.0	11.7	14.1	14.8	12.0	4.7	4.4	12.1	7.6	9.1	7.6	9.7	11.9	17.1	11.6	12.9
La	14.5	28.0	17.6	5.8	6.1	1.4	0.6	0.5	0.8	1.0	2.3	0.6	0.5	17.2	12.8	10.6	20.4
Ce	27.9	47.1	31.9	12.5	12.9	3.7	1.2	0.9	2.4	2.7	3.9	1.4	1.5	25.8	25.2	18.7	31.3
Pr	3.42	5.00	3.54	1.61	1.78	0.63	0.18	0.16	0.44	0.45	0.53	0.27	0.28	2.75	3.06	2.27	3.35
Nd	12.9	16.9	12.4	7.0	7.3	3.6	1.1	0.8	2.9	2.4	2.7	1.7	2.0	10.6	12.0	8.7	11.0
Sm	2.73	2.74	2.14	1.75	1.73	1.09	0.36	0.36	1.08	0.74	0.88	0.62	0.85	1.91	2.61	1.86	2.11
Eu	0.98	0.72	0.68	0.62	0.68	0.44	0.22	0.25	0.57	0.37	0.39	0.35	0.47	0.61	0.82	0.58	0.78
Gd	3.05	2.42	1.88	2.17	2.19	1.57	0.57	0.63	1.77	1.02	1.22	1.04	1.36	2.01	2.73	1.88	2.25
Tb	0.53	0.44	0.36	0.40	0.40	0.30	0.12	0.13	0.33	0.21	0.26	0.22	0.27	0.35	0.47	0.37	0.40
Dy	3.39	2.59	1.96	2.38	2.51	1.89	0.85	0.78	2.16	1.24	1.47	1.36	1.71	1.97	2.83	2.11	2.31
Ho	0.72	0.51	0.41	0.51	0.52	0.44	0.18	0.16	0.46	0.28	0.34	0.30	0.36	0.41	0.58	0.41	0.46
Er	2.05	1.73	1.34	1.48	1.53	1.27	0.50	0.46	1.34	0.74	0.99	0.83	0.99	1.32	1.66	1.23	1.45
Tm	0.35	0.33	0.26	0.23	0.24	0.19	0.08	0.07	0.20	0.14	0.18	0.14	0.15	0.23	0.25	0.22	0.26
Yb	2.29	2.10	1.54	1.55	1.52	1.21	0.50	0.46	1.24	0.75	0.91	0.78	0.93	1.43	1.66	1.25	1.59
Lu	0.34	0.36	0.26	0.23	0.23	0.19	0.07	0.06	0.18	0.12	0.15	0.12	0.13	0.24	0.25	0.21	0.26
Ba/Nb	36.46	47.44	87.84	44.19	30.63	28.75	70.00	40.00	45.00	24.00	40.00	65.00	77.78	60.38	59.53	32.73	67.26
La/Nb	1.46	1.59	1.52	1.87	1.91	1.75	3.00	2.50	4.00	2.00	4.60	3.00	5.56	2.21	1.49	1.20	1.92
La/Ta	29.0	20.0	16.0	29.0	30.5	14.0	6.7	6.3	11.4	11.1	25.6	7.5	5.0	57.3	16.0	13.3	34.0
Zr/Nb	12.59	10.80	15.94	19.65	10.13	19.50	42.50	18.00	95.5	29.60	35.60	39.50	94.44	14.36	8.86	6.74	12.30
Nb/U	5.21	4.51	3.41	3.88	8.00	8.00	2.00	2.00	2.00	5.00	2.50	2.00	4.00	2.52	4.78	3.14	2.72
Rb/Sr	0.32	0.19	0.15	0.02	0.06	0.01	0.00	0.01	0.01	0.01	0.04	0.01	0.01	0.10	0.05	0.03	0.10

◆;quartz monzodiorite, ■,diorite, ▼;quartz diorite, ●; tonalite, ○;granite, □;adamellite, ▲;syenite

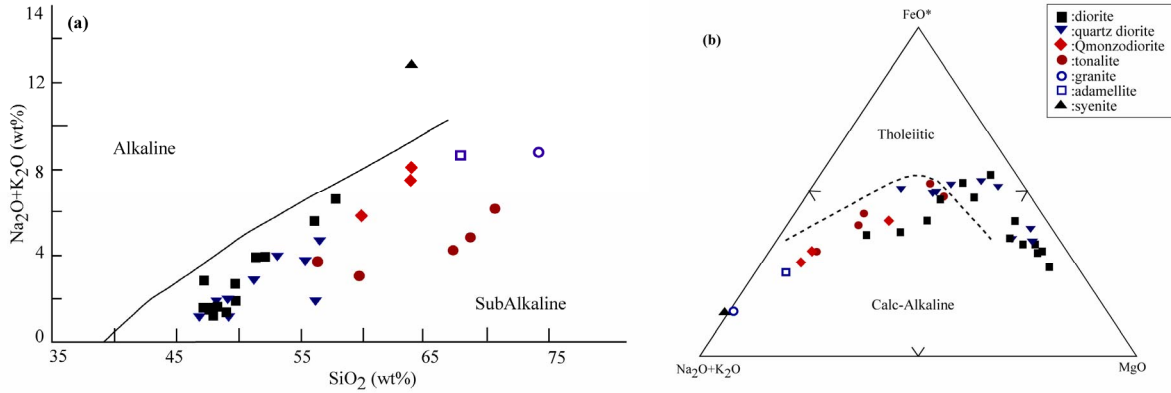


Figure 3. Major element geochemical discrimination diagrams of the Pertek granitoid. (a) Total alkalis vs silica [47]; dividing line between alkaline and subalkaline fields [48] (b) AFM triangular diagram [47].

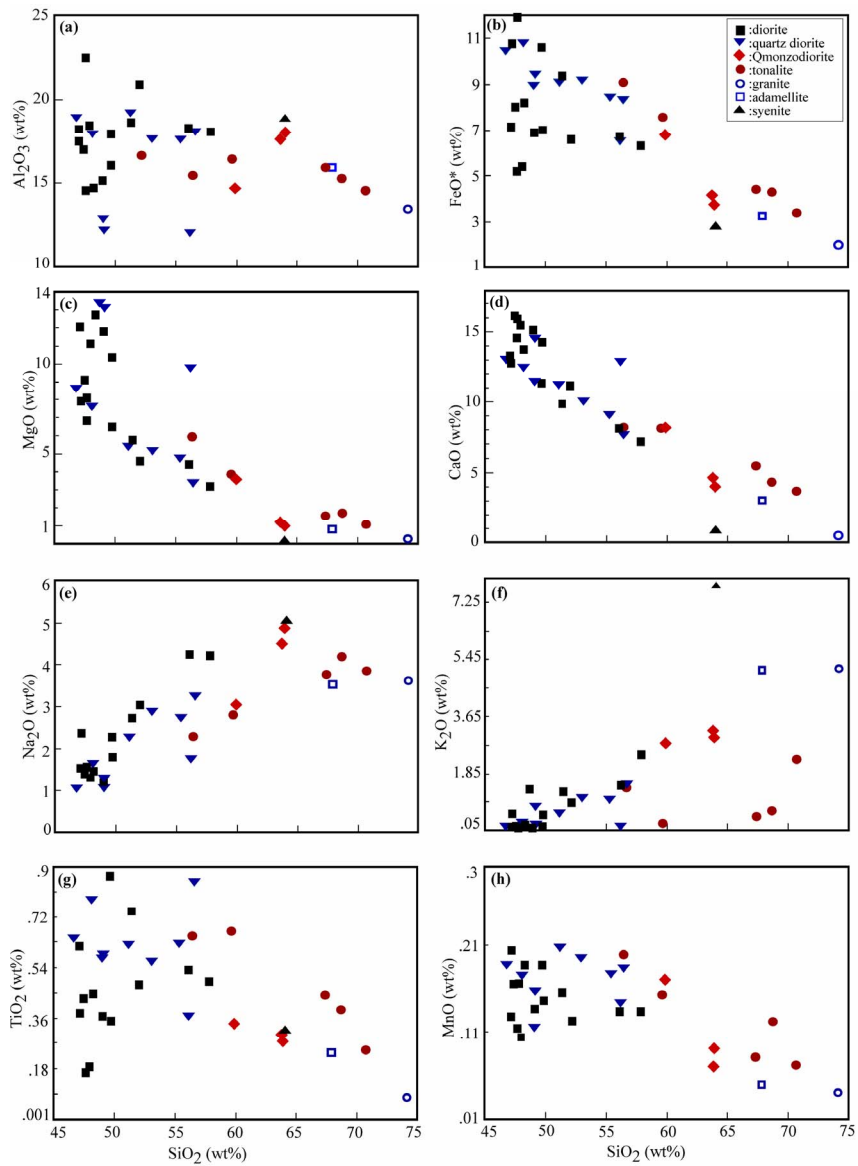


Figure 4. Major oxides vs. SiO₂ variation diagrams for rock samples from the Pertek granitoid.

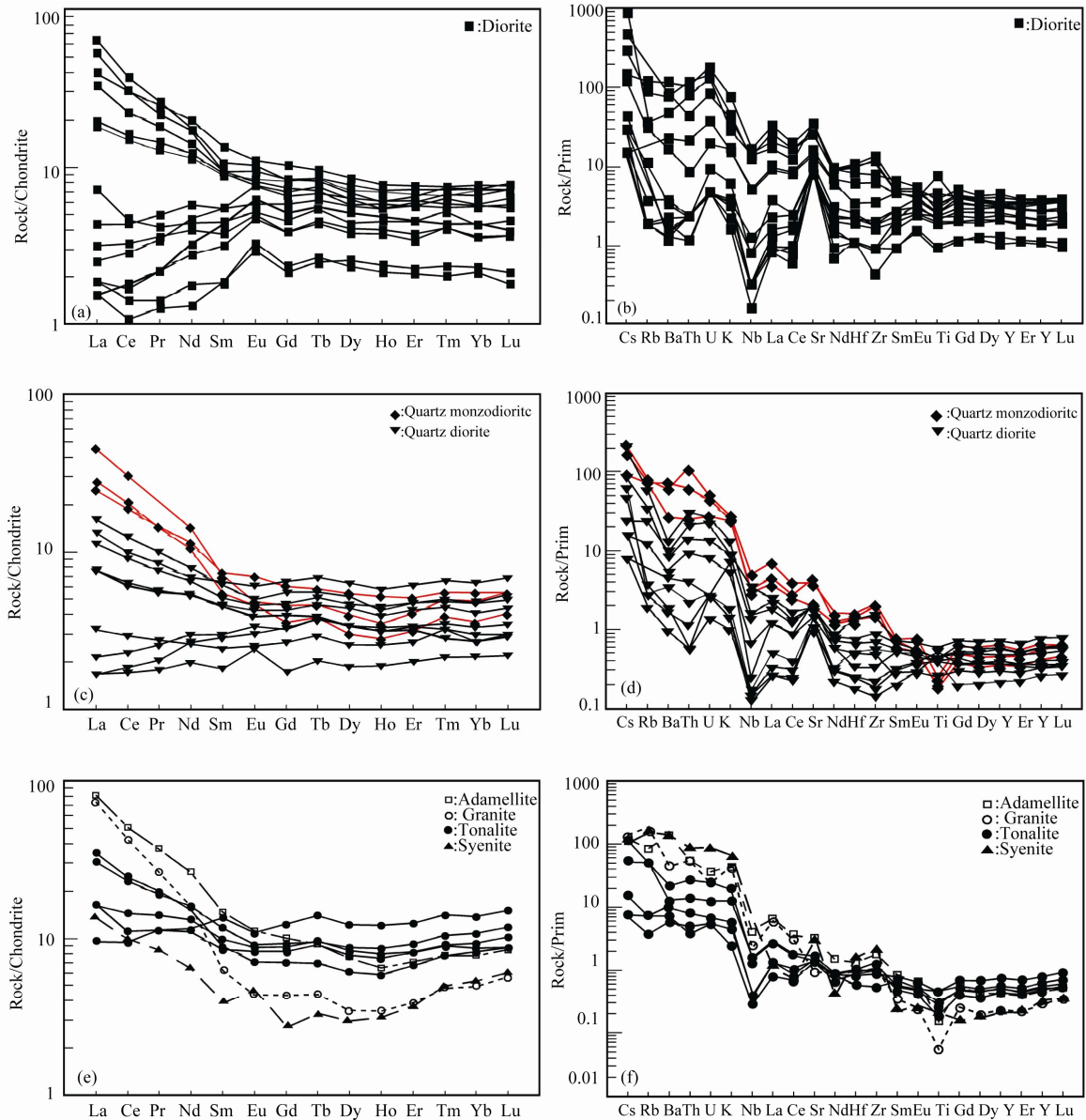


Figure 5. (a) Chondrite (b-c) PRIM normalized spider diagrams for the Pertek granitoid. (PRIM and Chondrite normalizing values after [49]).

a significant negative anomaly whereas Sr show, particularly in diorites and quartz diorites, a strong positive anomaly. Ti, in all different lithologies but particularly in tonalites, show a strong negative anomaly (**Figure 5(f)**). Medium and heavy REEs (Sm-Lu) are depleted in all rock types. When all the geochemical characteristics of the geographically close and mineralogically similar diorites are taken into consideration, this significant difference observed in spider diagrams do not seem to be caused by fractionation or fractional crystallization from a single magma source. Mixing of two different magma sources may explain these geochemical characteristics [30].

7. Petrogenesis

Fractional crystallization processes during crystallization of the Pertek granitoid is defined in Harker type major oxides-silica diagrams (**Figure 4**). In these diagrams a negative correlation in FeO^* , MgO , CaO , Ti_2O ve MnO ratios and a positive correlation in Na_2O and K_2O ratios with the increasing SiO_2 indicate the fractional crystallization. Particularly MgO ratios of 3% - 14 % in diorites and quartz diorites indicate that olivine and pyroxene played important role during the fractionation phase. In the other rock groups amphiboles accompanied olivine and pyroxene during fractionation. This fractionation

could be defined also in LILE and HFSE vs silica diagrams (Figure 6). For example, in quartz and quartz diorites Rb and Ba contents increase with the increasing silica (Figure 6(a) and (b)) indicating assimilation-fractional crystallization processes. Similarly in Sr-SiO₂, Y-Rb variation diagrams (Figure 6(c) and (d)), amphibole and bio-tite effect in diorites, quartz diorites and tonalites is clear.

Samples from the Pertek granitoid are plotted in chemical affinity diagram of Debon Le Fort [26] (Figure 7) (I, II, III are peraluminous, IV, V, VI are metaluminous in character), our samples in this diagram are plotted in areas of IV and V indicating metaluminous-cafemic character. However some samples including diorites, are found in leucogranites area. Autochthonous or intrusive granitoids of peraluminous character are related to the crustal source in collisional or post collisional tectonic setting. Metaluminous more basic rocks, on the other hand, are related to crust-mantle (hybrid) source in collisional or post collisional tectonic setting. Debon Le Fort [26] noted that aluminous magma suites generally were formed by the partial melting of sialic material and cafemic suites may evolve from mantle or, more com-

monly, a hybrid magma of mantle-sialic material mixing. Debon Le Fort [26] suggests cafemic character of magma suites indicate depletion in mantle source.

Ni composition is an important indicator in plutonic rocks in order to determine if the source was primitive or originated from depleted mantle. In tonalites and quartz monzodiorites of the Pertek granitoid, Ni composition varies from 15 to 24 ppm indicating that their source was not primitive mantle but may be a fractionally crystallized depleted mantle [34]. However, in diorites Ni ratio varies from 18 to 178 ppm and in quartz diorites from 17 to 112 ppm (Table 1) indicating that the more basic rocks might have evolved from primitive mantle. In addition to that, most of the acidic and basic samples are gathered in an area between MORB and subduction melt areas in La/Nb-Ti variation diagram (Figure 8(a)). In Th/Yb-Ta/Yb variation diagram they are found in subduction zone and N-type MORB areas and effect of fractional crystallization could be defined in diagram (Figure 8b). In the Zr/Yb-Nb/Yb diagram (Figure 8c) diorites are found in an area between depleted mantle (DM) or Oceanic Island Basalt (OIB) areas. Quartz diorites, in the same diagram, are gathered in Enrich-Ocean Ridge Basalt

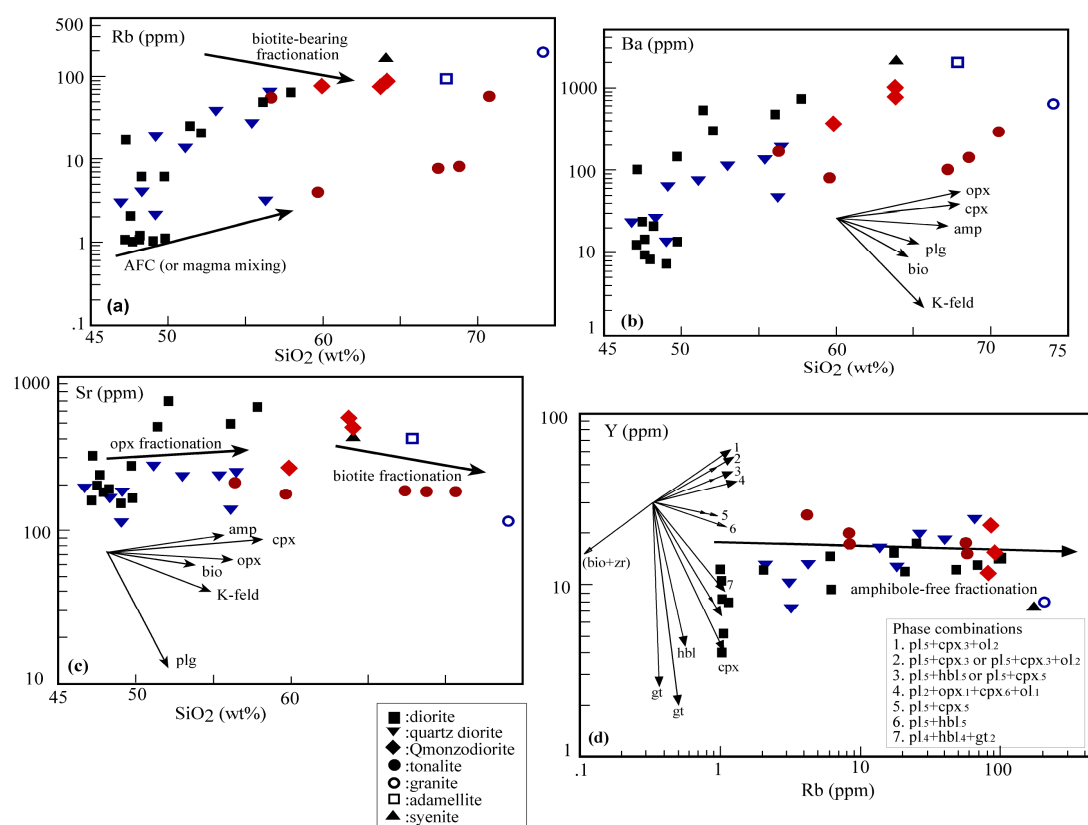


Figure 6. (a-c) Rb, Ba and Sr vs. silica semi-logarithmic variation diagrams of Pertek granitoid. (d) Y vs Rb. AFC; assimilation-fractional crystallisation, opx; orthopyroxene, cpx; clinopyroxene, amp; amphibole, plg; plagioclase, bio; biotite, K-feld; K-feldspar, hb; hornblende, gt; garnet, zr; zircon, ol; olivine.

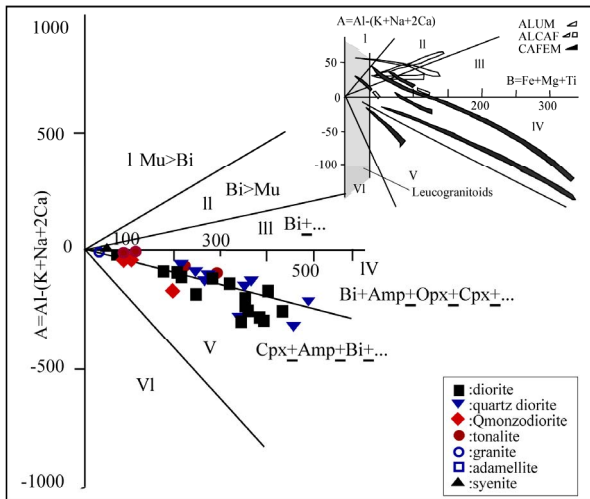


Figure 7. Chemical trends representing the main magma associations of the Pertek granitoid in the A-B characteristic minerals diagram [26]. I, II, III and IV, V, VI regions represent the peraluminous and metaluminous domains. Bi; biotite, mu; muscovite, hb; hornblende, opx; orthopyroxene, cpx; clinopyroxene, ol; olivine, ALUM; aluminous, ALCAF; aluminocafemic, CAFEM; cafemic association.

(E-MORB) area, and tonalites are found between DM and E-MORB areas. All samples are plotted in volcanic arc granitoid area in Nb-Y and Rb-Y/Nb variation diagrams (**Figure 9**). In Sm/Yb-Ce/Sm diagram, diorites are found in MORB area, and the others are in between MORB-OIB areas. Pearce et al. [35] noted that gathering in these areas might be caused by subduction zone enrichments of crustal contamination. Distribution of samples from the Pertek granitoid in Rb/Y-Nb/Y and Ba/Nb-La/Nb diagrams (**Figure 10(a-c)**) also show a crustal contributions into the magma.

As mentioned above, increasing in Rb/Sr and K_2O/P_2O_5 ratios with increasing SiO_2 is a clear indicator of crustal contamination (**Table 1**) [36]. However, this contamination should be considered with the assimilation-fractional crystallization (AFC) and partial melting [37]. Low La/Ta ratio also indicates crustal contamination [31]. When these interpretations are taken into consideration, these La/Ta ratios in diorites (La/Ta = 19.1), quartz diorite (La/Ta = 20.7) and quartz monzodiorite (La/Ta = 21.7) indicate effects of crustal contamination for these groups but tonalites (La/Ta = 38.7).

In some diagrams, given above, Pertek granitoid show similar geochemical composition to the mantle wedge. Considerably high Ba/Nb (11-139) and Zr/Nb (6-79) ratios (**Table 1**) indicate that these rocks were subjected to a mantle-sourced depletion [38]. Similarly, except for syenite (PR-31) and one quartz diorite sample, La/Nb ratios are higher than 1 and this also indicates that these groups evolved from a lithospheric mantle source [39]. It

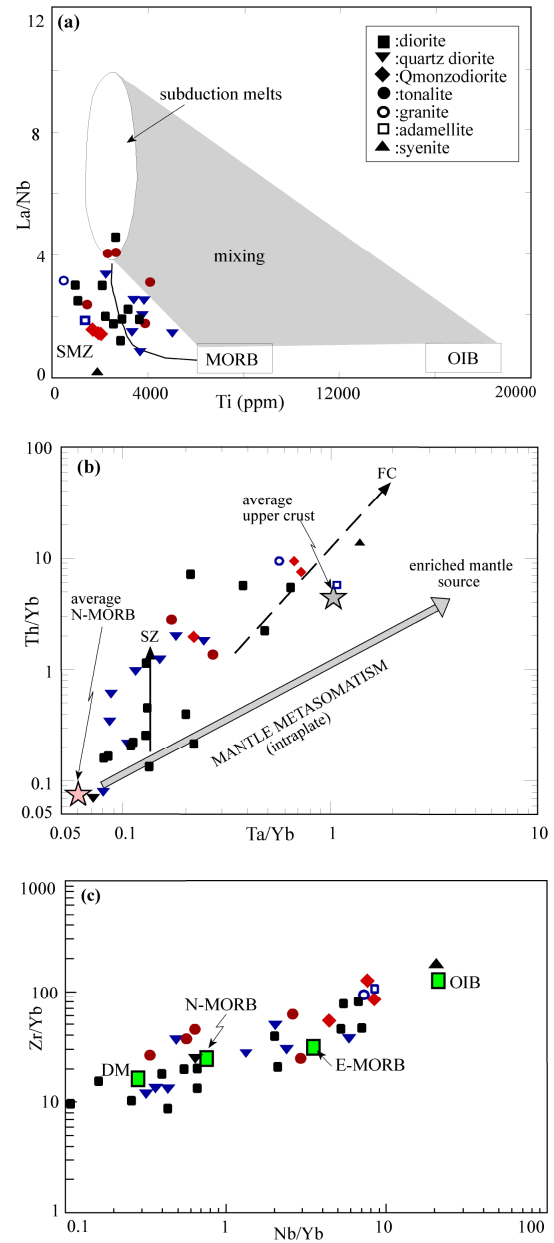


Figure 8. (a) La/Nb vs. Ti (ppm) [35]. (b) Th/Yb vs. Ta/Yb, [35] and (c) Zr/Yb vs. Nb/Yb plots of the rock samples from the Pertek granitoides. SMZ; subduction zone magmatites, MORB; Ocean Ridge Basalt, OIB; Ocean Island Basalt, FC; Fractional Crystallisation, DM; Depleted Mantle, N, E-MORB; Normal - Enrich Ocean Ridge Basalt.

is widely accepted that in subcontinental lithospheric mantle-sourced magma La/Nb is higher (La/Nb > 1) than asthenospheric mantle-sourced ones (La/Nb < 1) [39]. In Pertek granitoid samples La/Nb ratio varies from 1, 2 to 4, 6 indicating a lithospheric melt. However, some researchers also suggest that relative depletion in Nb and Ta might be caused by interaction between subcontinental lithospheric and asthenospheric melts [40].

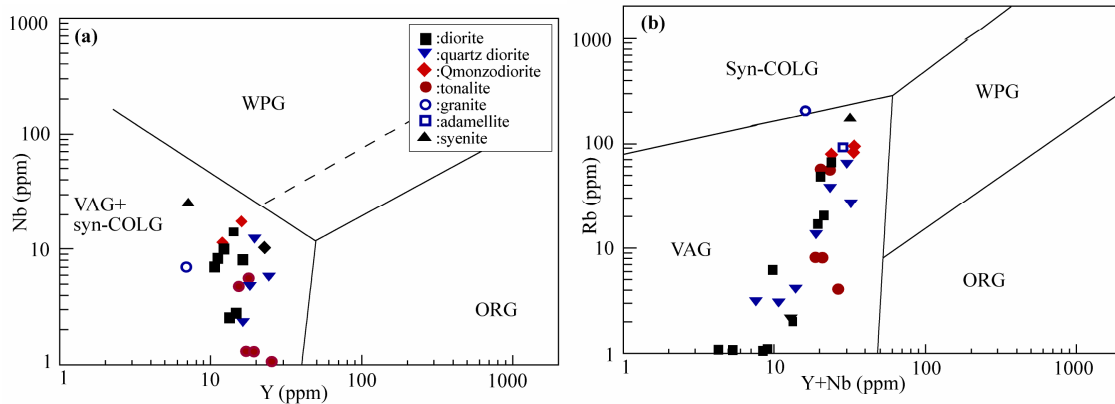


Figure 9. (a) Nb – Y and (b) Rb - Y+Nb [50] geotectonic discrimination diagrams for the Pertek granitoid. Syn COLG; Syn-Collisional Granitoid, WPG; Within-Plate Granitoid, VAG; Volcanic-Arc Granitoid, ORG; Ocean-Ridge Granitoid.

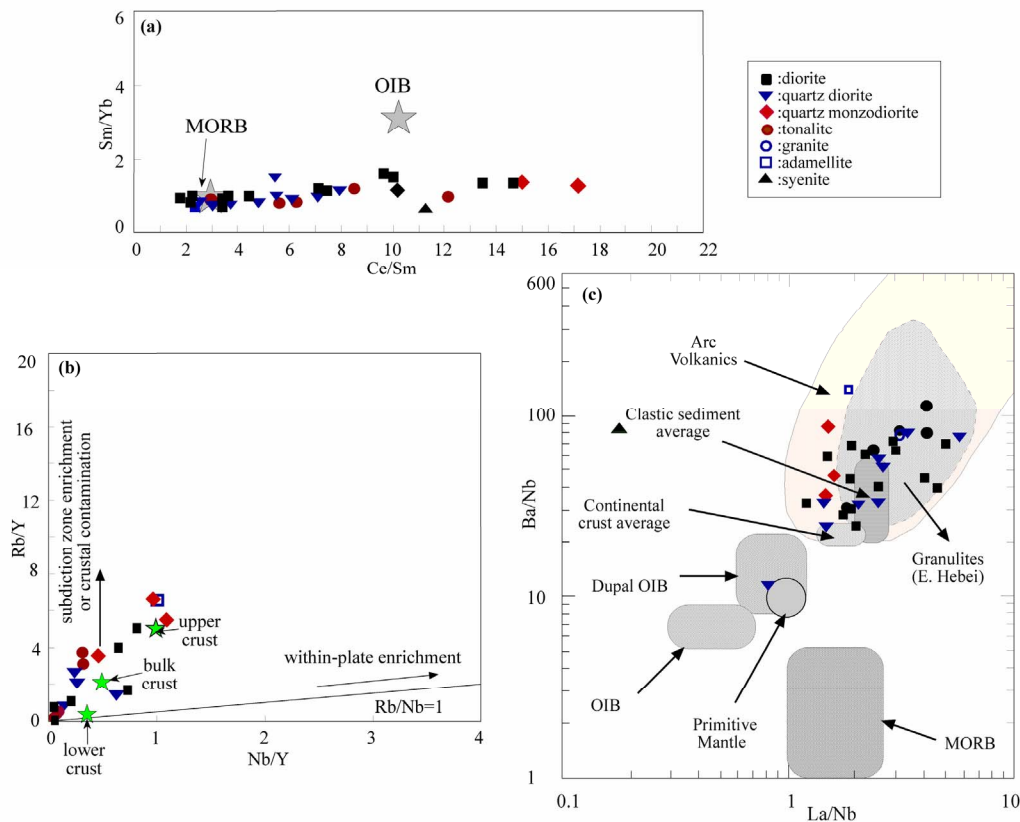


Figure 10. (a) Sm/Yb vs. Ce/Sm, (b) Rb/Y vs. Nb/Y [35], (c) Ba/Nb vs. La/Nb [51] plots of the rock samples from the Pertek granitoid.

8. Discussion and Conclusions

The NW-SE-trending Pertek granitoid consists of diorites, quartz diorites, quartz monzodiorites, tonalites and crosscutting aplites and monzonitic dykes that were all formed in similar tectonic setting. Large amount of mafic microgranular enclaves are found in quartz diorites, tonalites and monzonites. All these rocks, except for a

sample (PR-31) taken from syenites, are sub-alkaline; diorites and quartz diorites are tholeiitic and others are calc-alkaline in nature and all of them are evolved from a single phase magma during a normal crystallization process. Major element-silica variation characteristics show that fractionation particularly plagioclase, hornblende, pyroxene and olivine played an important role on their formation during a continuous crystallization period.

Table 2. The general features of the granitoides in the E-SE Anatolia.

	Rocks	Magma type	Tectonic setting	Age
Göksun-Afşin	Granodiorite and granitic [4]	Calc-alkaline [4]	Volcanic Arc [4]	85.76±3.17-77.49±1.91 [4]
Doğanşehir	Amphibole gabbro, diorite, quartz diorite, tonalite, granodiorite [43, 44]	I-type, peralüminus, calc-alkaline [43, 44]	Volcanic arc [43,44]	Compatible with the Baskil, Göksun-Afşin and Keban [4]
Baskil	Granite, granodiorite, tonalite, quartz monzonite, diorite, gabbro, aplite, diabase [2,16], granophyric, granite porphyre, granodiorite porphyre, microdiorite, quartz microdiorite, quartz diorite-porphyre, orbicular gabbro [2]	I-type [13], metalüminus, peralüminus [2,16], calc-alkaline [2] ± tholeiitic	Magmatic arc [14,45] Ensimatic island arc [3, 14] Volcanic arc granitoid [2]	Granitoid=81.5±1.1 [2] Diabase=78 my [16] Granite=76 ±2.5 – 78.5±2.5 my [8]
Keban	Tonalite, quartz diorite, gabbro, dacite, andesite, basalt [9,6,17]	Tonalites;calc-alkaline, I-type, metalüminus, peralüminus Diorite-gabbros; tholeiitic, M-type, metalüminus [17]	Volcanic Arc [17]	Tonalite=59.77 ± 1.2 -75.65 ± 1.5 Diorite= 84.76 ± 1.8 [17]
Pertek	Diorite, quartz diorite, Q.monzodiorite, tonalite, granite, syenite	I-type, metalüminus, Q.monzodiorite and tonalite; calc-alkaline, Diorite and Q.diorite; calc-alkaline and tholeiitic	Volcanic Arc Granitoid	68.6±5.6

Chontrite and pimordial mantle-normalized patterns of diorite and quartz diorites show two different path indicating that mantle-sourced magma that later formed the Pertek granitoid was enriched by fluids derived from the oceanic crust in an arc setting, and contaminated by continental crust. This result is supported by both the petrographic and geochemical evidences that magma formed in an arc setting, enriched by magmatic fluids derived from a subducted oceanic crust, injected into the crust and contaminetd in this crustal environment.

The repeated modifications in subcontinental lithospheric mantle by dehydration in subduction zones and accretionary prism sediments included by subcontinental lithospheric mantle [41] caused a relative depletion in Ti, Nb and Ta and an enrichment in Ba. The fact that the rocks are concentrated in classical sedimentary and granulite areas may indicate the same thing as well. Significant negative Nb and Ti anomalies in Pertek granitoid are probably caused by its subduction sediment content. Negative Ti anomaly may also indicate apatite and Fe-Ti oxides played important role on petrogenesis [42].

In the geological map of MTA [21], the Cretaceous magmatic rocks cropping out to the N and NE of Elazığ are defined as “ophiolites” and “unclassified magmatic rocks”. The Pertek granitoid crops out in a part of this region and when our conclusions are compared with the other granitoids cropping out in the region, it is seen that they display similar characteristics (Table 2). Thus, it might be concluded that the Pertek granitoid is the eastern continuation of Elbistan (Kahramanmaraş), Doğanşehir (Malatya), Baskil and Keban (Elazığ) granitoids.

The future petrographic and geochemical studies on the cross-cutting acidic dayks would contribute in under-

standing if the magmatism was bimodal in nature or not. In order to clarify the problems, related to the place and importance of the Pertek granitoid within the context of geotectonic evolution of the region, additional studies are needed along with the detailed geochemical studies we presented in this article. We continue studying isotop geochronology and isotop geochemistry of the Pertek granitoid in accordance with our purpose.

9. Acknowledgements

The authors gratefully acknowledge a grant from the University of Fırat, Project number FUBAP-1109 (Fırat University Scientific Research Projects Unit).

10. References

- [1] Y. Yılmaz, E. Yiğitbaş and S. C. Genç, “Ophiolitic and Metamorphic Assemblages of Southeast Anatolia and Their Significance in the Geological Evolution of the Orogenic Belt,” *Tectonics*, Vol. 12, No. 5, 1993, pp. 1280-1297. [doi:10.1029/93TC00597](https://doi.org/10.1029/93TC00597)
- [2] T. Rızaoğlu, O. Parlak, V. Höck, F. Koller, W. E. Hames and Z. Billor, “Andean Type Active Margin Formation in the Eastern Taurides: Geochemical and Geochronological Evidence from the Baskil Granitoid, SE Turkey,” *Tectonophysics*, Vol. 473, No. 1-2, 2009, pp.188-207. [doi:10.1016/j.tecto.2008.08.011](https://doi.org/10.1016/j.tecto.2008.08.011)
- [3] T. Rızaoğlu, O. Parlak and F. İşler, “Geochemistry and Tectonic Setting of the Kömürhan Ophiolite in Southeast Anatolia,” *5th International Symposium on Eastern Mediterranean Geology*, Thessaloniki, 14-20 April 2004, p. 285.
- [4] O. Parlak, “Geodynamic Significance of Granitoid Magmatism in the Southeast Anatolian Orogen: Geochemical

- and Geochronological Evidence from Göksun-Afşin (Kahramanmaraş, Turkey) Region,” *International Journal of Earth Sciences (Geologische Rundschau)*, Vol. 95, No. 4, 2006, pp. 609-627. [doi:10.1007/s00531-005-0058-2](https://doi.org/10.1007/s00531-005-0058-2)
- [5] G. Aktaş and A. H. F. Robertson, “The Maden Complex, SE Turkey: Evolution of a Neotethyan Continental Margin,” *Special Publications, London, Geological Society*, Vol. 17, No. 1, 1984, pp. 375-402. [doi:10.1144/GSL.SP.1984.017.01.27](https://doi.org/10.1144/GSL.SP.1984.017.01.27)
- [6] H. J. Asutay, “Baskil (Elazığ) Çevresinin Jeolojik Ve Petrografik İncelenmesi,” *MTA Dergisi*, Vol. 107, 1988, pp. 47-63.
- [7] A. F. Bingöl, “Petrographical and Petrological Features of Intrusive Rocks of Yüksekova Complex in the Elazığ Region (Eastern Taurus, Turkey),” *Journal of Fırat University Science and Technology*, Vol. 3, No. 2, 1988, pp. 1-17.
- [8] E. Yazgan and R. Chessex, “Geology and Tectonic Evolution of the South-Eastern Taurides in the Region of Malatya,” *Turkish Petroleum Geologists Bulletin*, 1991, Vol. 3, No. 1, pp. 1-42.
- [9] B. Akgül and A. F. Bingöl, “Piran (Keban) Köyü Çevresindeki Magmatik Kayaçların Petrografik ve Petrolojik Özellikleri,” *20th Yıl Jeoloji Sempozyumu, Bildiri Özleri*, 1997, pp. 79-80.
- [10] A. Önal and A. F. Bingöl, “Geochemical Characterisation and Petrogenesis of the Polat Granitoid in Eastern Taurus Belt, Turkey,” *Journal Geological Society of India*, Vol. 56, No. 3, 2000, pp. 235-251.
- [11] N. Düzgören-Aydın, W. Malpas, M. C. Göncüoğlu and A. Erler, “Post Collisional Magmatism in Central Anatolia, Turkey: Field, Petrographic and Geochemical Constraints,” *International Geology Review*, Vol. 43, No. 8, 2001, pp. 695-710.
- [12] O. Parlak and T. Rızaoğlu, “Geodynamic Significance of Graitoid Intrusions in the Southeast Anatolian Orogeny (Turkey),” *Proceedings of the 5th International Eastern Mediterranean Geological Symposium*, Thessaloniki, 2004, pp. 14-20.
- [13] T. Rızaoğlu, O. Parlak and F. İşler, “Geochemistry and Tectonic Significance of Esence Granitoid (Göksun-Kahramanmaraş), SE Turkey,” *Yerbilimleri*, 2005, Vol. 26, pp.1-13.
- [14] A. H. F. Robertson, O. Parlak, T. Rızaoğlu, U. C. Ünlügenç, N. İnan, K. Taşlı and T. Ustaömer, “Late Cretaceous-Mid Tertiary Tectonic Evolution of the Eastern Taurus Mountains and Southern Tethyan Ocean Evidence from the Elazığ Region, SE Turkey,” *Geological Society of London Special Publication*, 2006, Vol. 272, pp. 231-270.
- [15] A. H. F. Robertson, O. Parlak, T. Rızaoğlu, U. C. Ünlügenç, N. İnan, K. Taşlı and T. Ustaömer, “Tectonic Evolution of the South Tethyan Ocean: Evidence from the Eastern Taurus Mountains (Elazığ region, SE Turkey),” *Special Publications, Geological Society*, 2007, Vol. 272, pp. 233-272.
- [16] A. Önal, “K-Ar Cooling Age, Whole-Rock and Pb-Sr İso-Topo Geochemistry of Baskil Granitoid,” *International Participation, 61th Geological Congress of Turkey*, Ankara, 2008, pp. 110-111.
- [17] S. Kürüm, “Keban (Elazığ) Yöresi Plutonik Kayaçlarında K/Ar Radyometrik Yaşı ve Sr-Pb İzotop Jeokimyası,” *61th Türkiye Jeoloji Kurultayı Bildiri Özleri, Bildiri Özleri*, 2008, pp. 112-113.
- [18] M. Ural and S. Kürüm, “Microscopic and Diffractometric Studies Inferred from Skarn Zonations between the Keban Metamorphites and Elazığ Magmatites, Around Elazığ,” *Fırat Üniversitesi Turkish Journal of Science & Technology (IJST)*, Vol. 4, No. 2, 2009, pp. 87-102.
- [19] E. Aksoy, “Pertek (Tunceli) Çevresinin Jeolojik Özellikleri ve Pertek Bindirme Fayı,” *Fırat Üniversitesi Fen ve Mühendislik Bilimleri Dergisi*, Vol. 6, No. 2, 1994, pp. 1-8.
- [20] S. Kürüm and A. F. Bingöl, “Elazığ Yakın Kuzey-Batısındaki Volkanitlerin Petrolojik Özellikleri,” *Fırat Üniversitesi Fen ve Mühendislik Bilimleri Dergisi*, Vol. 8, No. 2, 1996, pp. 83-98.
- [21] MTA, 1/500.000 “Türkiye Jeoloji Haritası,” General Directorate of Mineral Research and Exploration, Ankara, 2002.
- [22] E. Yazgan, “Geodynamics Evolution of the Eastern Taurus Region,” *Proceedings of International Symposium on the Geology of the Taurus Belt*, Ankara, 1984, pp. 199-208.
- [23] E. Kipman, “Keban Volkanitlerinin Petrolojisi,” *İstanbul Üniversitesi Yer Bilimleri Dergisi*, Vol. 3, No. 4, 1983, pp. 205-230.
- [24] N. Özgül and A. Turşucu, “Stratigraphy of the Mesozoic Carbonate Sequence of the Munzur Mountains (Eastern Taurus),” *Int Symposium on the Geology of Taurus Belt*, 1984, pp. 173-180.
- [25] M. Altunbey and H. Çelebi, “Kanatburun (Pertek-Tunceli) Yöresindeki Skarn Kayaçlarının Mineralojik ve Jeokimyasal Özellikleri,” *Selçuk Üniversitesi Mühendislik Mimarlık Fakültesi jeoloji Mühendisliği Bölümü 20 Yıl Jeoloji Sempozyumu Bildiriler*, 1997, pp. 45-58.
- [26] F. Debon and P. Le Fort, “A Chemical-Mineralogical Classification of Common Plutonic Rocks and Associations,” *Transactions of the Royal Society of Edinburgh: Earth Sciences*, Vol. 73, No. 3, 1983, pp. 135-149.
- [27] A. Streckeisen, “To Each Plutonic Rock Its Proper Name,” *Earth-Science Reviews*, Vol. 12, No. 1, 1976, pp. 1-33. [doi:10.1016/0012-8252\(76\)90052-0](https://doi.org/10.1016/0012-8252(76)90052-0)
- [28] M. J. Hibbard, “Textural Anatomy of Twelve Magma-Mixed Granitoid Systems,” In: J. Didier and B. Barbarin, Eds., *Enclaves and Granite Petrology. Developments in Petrology*, Vol. 13, 1991, pp. 431-444.
- [29] A. J. R. White and B. W. Chappell, “Some Supracrustal (S-Type) Granites of the Lachlan Fold Belt,” *Transactions of the Royal Society of Edinburgh: Earth Sciences*, Vol. 79, 1988, pp. 169-181.
- [30] H. R. Rollinson, “Using Geochemical Data: Evaluation, Presentation, Interpretation,” *Longman Scientific and Technical*, Wiley, New York, 1993, p. 352.
- [31] M. C. Göncüoğlu, K. Sayit and U. K. Tekin, “Oceani-

- zation of the Northern Neotethys: Geochemical Evidence from Ophiolitic Melange Basalts within the İzmir-Ankara Suture Belt, NW Turkey,” *Lithos*, Vol. 116, No. 1-2, 2010, pp. 175-187.
- [32] J. A. Pearce, “Role of the Subcontinental Lithosphere in Magma Genesis at Continental Margins,” In: C. J. Hawkesworth and M. J. Norry, Eds., *Continental Basalts and Mantle Xenoliths*, Shiva Publishing, Cheshire, 1983, pp. 230-249.
- [33] J. A. Pearce, “Trace Element Characteristics of Lavas from Destructive Plate Boundaries,” In: R. S. Thorpe, Ed., *Andesites, Orogenic Andesites and Related Rocks*, Wiley, Chichester, 1982, pp. 525-548.
- [34] A. Machado, E. F. Lima, F. J. Chemale, et al., “Geochemistry Constraints of Mesozoic-Cenozoic Calc-Alkaline Magmatism in the South Shetland Arc, Antarctica,” *Journal of South American Earth Sciences*, Vol. 18, No. 3-4, 2005, pp. 407-425. [doi:10.1016/j.jsames.2004.11.011](https://doi.org/10.1016/j.jsames.2004.11.011)
- [35] J. A. Pearce, J. F. Bender, S. E. De Long, W. S. F. Kidd, P. J. Low, Y. Güner, F. Şaroğlu, et al., “Genesis of Collision Volcanism in Eastern Anatolia, Turkey,” *Journal of Volcanology and Geothermal Research*, Vol. 44, No. 1-2, 1990, pp. 189-229. [doi:10.1016/0377-0273\(90\)90018-B](https://doi.org/10.1016/0377-0273(90)90018-B)
- [36] R. W. Carlson and W. K. Hart, “Flood Basalt Volcanism in the Pacific Northwestern United States,” In: J. D. Maccougal, Ed., *Continental Flood Basalts*, Kluwer, 1988, pp. 35-62.
- [37] D. J. De Paolo, “Trace Element and Isotopic Effects of Combined Wallrock Assimilation and Fractional Crystallization,” *Earth and Planetary Science Letters*, Vol. 53, No. 2, 1981, pp. 189-202. [doi:10.1016/0012-821X\(81\)90153-9](https://doi.org/10.1016/0012-821X(81)90153-9)
- [38] R. J. Stern, “Subduction Zones,” *Reviews of Geophysics*, Vol. 40, No. 4, 2002, pp. 10-12. [doi:10.1029/2001RG000108](https://doi.org/10.1029/2001RG000108)
- [39] J. G. Fitton, D. James and W. P. Leeman, “Basic Magmatism Associated with Late Cenozoic Extension in the Western United States: Compositional Variation In-Space and Time: The Temporal and Spatial Association of Magmatism and Metamorphic Core Complexes,” *Journal of Geophysical Research*, Vol. 96, No. 13, 1991, pp. 693-711.
- [40] P. B. Kelemen, K. T. M. Johnson, R. J. Kinzler and A. J. Irving, “High-Field-Strength Element Depletions in Arc Basalts Due to Mantle-Magma Interaction,” *Nature*, Vol. 345, No. 6275, 1990, pp. 521-524.
- [41] S. S. Sun and W. F. McGonough, “Chemical and Isotopic Systematics of Oceanic Basalts: Implications for Mantle Composition and Processes,” In A. D. Saunders and M. J. Norry, Eds., *Magmatism in the Ocean Basins, Geological Society Special Publication*, Vol. 42, 1989, pp. 313-345.
- [42] B. Villemant, H. Jaffrezic, J. L. Joron, et al., “Distribution Coefficients of Major and Trace Elements: Fractional Crystallization in the Alkalibasalt Series of Chaîne du Puy (Massif Central, France),” *Geochimica et Cosmochimica Acta*, 1981, Vol. 45, No. 11, pp. 1997-2016. [doi:10.1016/0016-7037\(81\)90055-7](https://doi.org/10.1016/0016-7037(81)90055-7)
- [43] F. Karaoğlu, “Günedoğru-Beğre (Doğanşehir—Malatya) Arasında Yüzeyleyen Tektono-Magmatik Birimlerin Petro- Grafisi ve Jeokimyası,” MSc Thesis, Çukurova University, Adana, 2005.
- [44] F. Karaoğlu and O. Parlak, “Geochemistry and Tectonic Significance of the Doğanşehir (Malatya) Granitoid,” *Abstracts of the 59th Geological Congress of Turkey*, 20-24 March 2006, Ankara, pp. 495-496.
- [45] M. Beyarslan and A. F. Bingöl, “Petrology of a Supra-Subduction Zone Ophiolite (Elazığ, Turkey),” *Canadian Journal of Earth Sciences*, Vol. 37, No. 10, 2000, pp. 1411-1424. [doi:10.1139/e00-041](https://doi.org/10.1139/e00-041)
- [46] A. Öztüfekçi Önal, D. Boztuğ, S. Kürüm and B. Akgül, “Pertek İntrüzif Kayaçlarında İzotopik ve Jeokimyasal Veriler, Doğu Anadolu, Türkiye,” *4th Ulusal Jeokimya Sempozyumu*, Bildiri Özleri, 2010, pp. 49-50.
- [47] T. N. Irvine and W. R. A. Baragar, “A Guide to the Chemical Classification of Common Volcanic Rocks,” *Canadian Journal of Earth Sciences*, 1971, Vol. 8, No. 5, pp. 523-548. [doi:10.1139/e71-055](https://doi.org/10.1139/e71-055)
- [48] P. C. Rickwood, “Boundary Lines within Petrologic Diagrams Which Use Oxides of Major and Minor Elements,” *Lithos*, Vol. 22, No. 4, 1989, pp. 247-263. [doi:10.1016/0024-4937\(89\)90028-5](https://doi.org/10.1016/0024-4937(89)90028-5)
- [49] S. S. Sun, “Chemical Composition and Origin of the Earth’s Primitive Mantle,” *Geochimica et Cosmochimica Acta*, Vol. 46, No. 2, 1982, pp. 179-192. [doi:10.1016/0016-7037\(82\)90245-9](https://doi.org/10.1016/0016-7037(82)90245-9)
- [50] J. A. Pearce, N. B. W. Harris and A. G. W. Tindle, “Trace Element Discrimination Diagrams for the Tectonic Interpretation of Granitic Rocks,” *Journal of Petrology*, Vol. 25, No. 4, 1984, pp. 956-983.
- [51] B. M. Jahn, F. Wu, C. H. Lo and C. H. Tsai, “Crust-Mantle Interaction Induced by Deep Subduction of the Continental Crust: Geochemical and Sr-Nd Isotopic Evidence from Post-Collisional Mafic-Ultramafic Intrusions of the Northern Dabie Complex, Central China,” *Chemical Geology*, 1999, Vol. 157, No. 1, pp. 119-146. [doi:10.1016/S0009-2541\(98\)00197-1](https://doi.org/10.1016/S0009-2541(98)00197-1)